Excitonic Optical Tamm States: a step towards a full molecular-dielectric photonic integration

S. Núñez-Sánchez[1,2], M. López-García[2], M. M. Murshidy[3,4], A. G. Abdel-Hady[5], M. Y. Serry[6], A. M. Adawi[3], J.G. Rarity[2], R. Oulton[2,7], W.L. Barnes[1]

School of Physics and Astronomy, University of Exeter, UK[1]

Photonics Group, Department of Electrical and Electronic Engineering, University of Bristol, UK[2]

Department of Physics and Mathematics, University of Hull, UK[3]

Department of Physics, Faculty of Science, Helwan University, Helwan, Egypt[4]

Yousef Jameel Science and Technology Research Center, The American University in Cairo, Egypt[5]

Department of Mechanical Engineering, The American University in Cairo, Egypt[6]

School of Physics, University of Bristol, UK[7]

Abstract

We report the first experimental observation of an Excitonic Optical Tamm State supported at the interface between a periodic multilayer dielectric structure and an organic dye-doped polymer layer. The existence of such states is enabled by the metal-like optical properties of the excitonic layer based on aggregated dye molecules. Experimentally determined dispersion curves, together with simulated data, including field profiles, allow us to identify the nature of these new modes. Our results demonstrate the potential of organic excitonic materials as a powerful means to control light at the nanoscale, offering the prospect of a new alternative photonic building block for nanophotonics designs based on molecular materials.

Graphical Table of Contents (TOC)

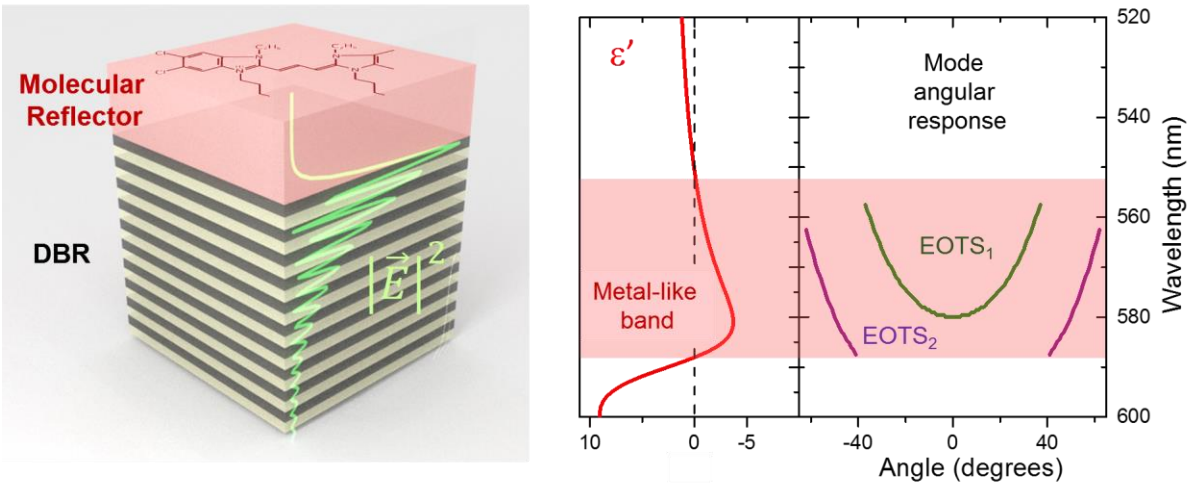

Keywords: Exciton, Surface modes, Tamm states, J-aggregates, Thin films, Organic, Molecular materials, Plasmons.

PACS : 78.67.Pt, 42.25.Bs, 73.20.Mf, 42.70.Jk

Controlling light beyond the diffraction limit is now a routine matter, and is primarily achieved in the visible and near infrared part of the electromagnetic spectrum by making use of the plasmon modes associated with metallic nanostructures [1]. The key advantages that resonant plasmon modes bring are enhanced electromagnetic field strengths and sub-wavelength field confinement with, for example, a number of strong potential applications in areas such as quantum technology[2]. A number of alternatives to metals have now been explored [3–5], including graphene[6] and other atomically thin materials [7]. Very recently interest has been rekindled in using molecular resonances, especially in the form of molecular excitonic states [8,9]. Such materials may exhibit a strong enough resonant excitonic response that the real part of the associated permittivity becomes negative in the vicinity of the

resonance. When this happens the excitonic material may take on a reflective, metallic appearance [10,11]. Early work in this area involved molecular crystals, for which a negative real permittivity was achieved at low temperatures [12]. In the 1970s Philpott and co-workers showed that organic excitonic crystals may support surface exciton-polaritons [12,13], analogous to the surface plasmon-polaritons supported by metals[14]. Recently surface exciton-polaritons supported by dye-doped polymers have been experimentally demonstrated[8,9], and localized (particle-like) exciton-polaritons theoretically predicted [8,15,16]. Here we provide the first demonstration that molecular materials can also be used as building blocks to create another class of nanophotonic mode, specifically Optical Tamm States (OTSs). By extending the range of nanophotonic modes supported by molecular materials, our results open the exciting the prospect of using molecular materials to replace metals as a means to control light at the nanoscale in an integrated fully-dielectric scheme[17].

OTSs are optical modes that occur at the interface between two reflective photonic structures[18], with fields that decay with distance from the interface that supports them. Demonstration of the existence of these modes has previously been performed using two periodic dielectric stacks[18], or a combination of a periodic dielectric stack and a metallic reflector[19]. When the reflector is a metal thin film the modes are named Tamm plasmons which have shown potential applications as: sensors[20], lasers with enhanced directional emission [21,22] and for control of spontaneous optical emission of single photon emitters[23]. Control of polarization and angular response has been obtained by using pattern processing to impose nanostructure on the metallic reflector layer [22,24] in order to confine laterally the modes [23]. Here we show that OTSs with a tailored dispersion curve can also occur between a periodic dielectric stack and an organic (molecular) reflector thin film, giving a new class of OTS mode, an Excitonic Optical Tamm State (EOTS). The limited wavelength range over which metal-like reflectance occurs for the excitonic layer defines a truncated dispersion of the EOTS modes without the need for patterning of the excitonic layer.

In this Letter we demonstrate the existence of EOTS modes between a truncated 1-D photonic crystal (Distributed Bragg Mirror-DBR) and a polymer layer heavily doped by J-aggregate molecules (the excitonic layer). Light may excite an EOTS when illumination takes place at an incident angle that allows momentum matching to the EOTS to be achieved. The spectrally narrow range over which the metal-like behaviour occurs limits the spectral range over which EOTS may be supported. Below we demonstrate that one can tailor the EOTS dispersion curve and its cut-off wavelengths through the overlap of the momentum-matching mode condition and the limited wavelength range of metal-like properties of the excitonic layer. In what follows, we first describe the characteristic dispersion curves associated with the EOTS based on the optical properties of our excitonic material and on the DBR stopband position. We then present an experimental observation of EOTS excitation in three photonic structures, each showing a different mode cut-off wavelength.

The propagation condition for an OTS in a multilayer structure DBR/(thin film) requires that the thin film shows a high reflectivity response within the stop-band of the DBR stack[19]. In the visible metals such as silver can fulfil this condition over the entire visible wavelength range. A dielectric medium doped with an excitonic species exhibiting a strong absorption resonance may be modelled using the classical single Lorentz oscillator model,

$$\epsilon_r(\omega) = 1 + \chi(\omega) + \frac{f_0\omega_0^2}{\omega_0^2 + \omega^2 + i\gamma_0\omega}$$

where the resonance frequency (ω_0) corresponds to the exciton transition, γ_0 is the damping rate, and $f_0$is the reduced oscillator strength; the term χ takes into account the background susceptibility whilst the reduced oscillator strength is proportional to the concentration of excitonic species. If the oscillator strength is strong enough then the real part of the permittivity will take negative values over a limited wavelength range, giving a coloured metallic lustre to the organic layer [10,11]. In this work we take the values for the resonance frequency, the damping parameter, and background susceptibility from previous work [8]. For our theoretical study we first considered an excitonic layer with a value of the reduced oscillator strength

around unity. Using this oscillator strength, the real part of the permittivity attains negative values over a wavelength band of 100 nm centred on the short wavelength side of the excitonic transition (from 490 nm to just below 590 nm). The excitonic layer fulfils the condition of high reflectance only in this wavelength range (see supplementary information, section 1). For the DBR structure we considered a stack formed of 9 pairs of silicon oxide and silicon nitride layers, similar to our experimental samples, but with a central wavelength of 490 nm. The stopband edge of this DBR at normal incidence lies within the high reflectance wavelength band of the excitonic layer.

Figure 1.a shows the simulated P-polarized reflectance (TM) at normal incidence of the DBR stack and two photonic structures supporting OTS, a DBR/(excitonic layer) that supports an EOTS mode and a DBR/(silver layer) that supports a Tamm Plasmon Mode (TP). The DBR shows a high reflectance close to 100 % in the stopband range. However, in the two OTS structures we can observe a sharp dip in the reflectance when the condition of mode excitation is fulfilled. This condition is always observed to occur below the stopband edge of the DBR. If we compare the response of the TP structure with the EOTS structure, we observe that in the case of the TP structure the reflectance is close to unity over the whole wavelength range except when the mode is excited. This high reflectance is due to the mirror properties of the silver layer over all of the wavelength range examined. However, in structures supporting EOTSs, reflectance follows the individual DBR response outside the metal-like range of the excitonic material, showing a sharp dip only when the mode condition is achieved. This is because the high reflectance band of the excitonic layer occurs only over a limited wavelength range, outside this wavelength range the excitonic layer behaves as a simple dielectric without significantly affecting the DBR response, although the presence of this dielectric layer shifts the Fabry Perot oscillations associated with the DBR to longer wavelengths when compared to the response of the DBR alone.

To confirm the nature of the EOTS mode we need to examine the field intensity profile characteristic of an OTS. Figure 1.b shows the field intensity profile obtained for the TP mode,

it is seen to oscillate and to decay with distance away from the interface between the metal and the DBR stack. The decay profile within the DBR is modulated by the periodic variation of the refractive index of the DBR whilst it decays smoothly into the metal medium. Comparing Figure 1.b and Figure 1.c, the electric field profile obtained for the EOTS shows the same features as the TP, confirming that the EOTS has a field confinement that is similar to the TP. In order to confirm that the field profile is only due to the presence of excitonic species embedded in the polymer, we have calculated the field profile at the same illumination conditions (wavelength and angle) for a DBR stack covered by an organic thin film layer but with a null oscillator strength. The field intensity profile that we obtain is an oscillatory field that increases with distance away from the interface between the dielectric film and the DBR stack (see Figure 1.d), as is expected when an interference effect is responsible for the high reflectance in the stopband of the DBR stack [25].

Due to the similarities of the TP and EOTS, the dispersion curves of these modes have some properties in common. A TP is always located close to the low-energy stopband-edge[19]. We can thus use this low-energy stopband-edge to estimate the dispersion curves (see details in supplementary information, section 2). Note that the stopband-edge positions of a DBR stack depend strongly on the polarization and in-plane component of the wavevector. We thus expect that the mode condition should follow a similar trend to that of the DBR stopband edges. In the case of a TP structure, the mode condition can be met across all of the visible wavelength range, however, the EOTS excitation is necessarily limited to the region where the excitonic layer has permittivity values sufficiently negative to obtain a metal-like reflectance. Consequently the TP shows a continuous dispersion curve while the dispersion curves of the EOTS are truncated. These results show that it may be possible to design EOTS modes that can only be excited at normal incidence (zero-in plane component of the wavevector) or for a finite range of in plane components of the wavevector corresponding to oblique propagation. The truncation (cut-off) wavelengths are delimited by the convolution of

the low-energy stopband-edge of the DBR and the metal-like reflectance band of the excitonic layer.

Figure 2 shows the dispersion curves obtained for TP and EOTS in structures formed by two different DBR stacks (of central wavelengths 490 nm and 590 nm) with silver and an excitonic (TDBC) reflector. While the TP modes are allowed for all values of the in-plane component of the wavevector in the two different multilayer structures, the EOTS can only be excited over restricted illumination conditions. In the structure with a DBR with a central wavelength around 490 nm we can only excite modes near normal incidence ($k_{||}$=0), whilst for the structure with a DBR central of 590 nm the EOTS mode can only be excited by light impinging close to grazing incidence (large $k_{||}$ values). Therefore, by simply controlling the position of the DBR low-energy stopband-edge relative to the optical properties of the excitonic medium, it is possible to obtain an optical device with a controlled directional response without the need for surface nanostructure.

Three different multilayer structures supporting EOTS were fabricated using different DBR structures but with the same excitonic layer. The DBR mirrors were fabricated using 9 pairs of silicon dioxide and silicon nitride layers deposited by plasma enhanced chemical vapour deposition. The mirrors were designed with central wavelengths (λ_C) lying in the range 500 nm to 585 nm (DBR-500, DBR-520, DBR-585). The highly reflective excitonic layers were spin cast on top of the DBR mirrors from solutions of the molecular dye TDBC and poly(vinyl alcohol) (PVA) in water. Here we used TDBC molecules as excitonic species (5,6- dichloro-2-[[5,6-dichloro-1-ethyl-3-(4-sulphobutyl)-benzimidazol-2-ylidene]-propenyl]-1-ethyl-3-(sulphobutyl)-benzimidazolium hydroxide, sodium salt, inner salt), with an associated excitonic resonance centred at a wavelength of 590 nm. In appropriate solutions these molecules form J-aggregates; the excitons delocalize in such aggregates leading to (i) a stronger effective dipole moment associated with the exciton, and (ii) a narrower excitonic resonance (arising from exchange narrowing) [26] . This strong dipole moment makes these systems well suited to our purpose since this helps produce an optical response that is strong enough to exhibit a

negative permittivity. The TDBC-PVA solutions were prepared by mixing a PVA-water solution with TDBC-water solution as explained elsewhere[8]. All TDBC/PVA spun films deposited were designed to yield a 200 nm thickness for the excitonic layer. The optical properties and oscillator parameters of the TDBC/PVA layer were determined in a previous work through reflection and transmission spectroscopy of TDBC/PVA films spun on glass at normal incidence[8].

Angle and polarization resolved reflection maps of the compound structures were obtained using Fourier imaging spectroscopy (FIS) [27]. The samples were illuminated by projecting the output of a fibre coupled to a white light source (Thorlabs OS-L1) through a high numerical aperture objective lens Zeiss 63X ApoFluor (NA=0.75). The reflected pattern generated at the back focal plane of the objective was then scanned with a fibre coupled to a spectrometer (Ocean200+) so as to obtain the angle and polarization resolved reflectance of the structure for all angles within the NA of the objective lens ($\theta^{max}=48^0$ in our case). Angles were then translated into in-plane components of the incident wavevector ($k_{||}$) for comparison with the calculated dispersion curves.

Figure 3 shows the experimental reflectance maps for P-polarized light as a function of energy and in-plane wavevector for three different EOTS structures. Theoretical dispersion curves are plotted on top of the experimental results to visualize the cut-off wavelengths for the different combination of DBRs and the excitonic layer. EOTS are supported by all the three structures. For the multilayer structure comprising a DBR with a central wavelength of 500 nm the EOTS could be only excited for incidence angles below 36 degrees ($k_{||}$~4.7 um^{-1}). The dip in the reflectance observed at large wave vectors corresponds to the DBR band edge and not to the presence of an EOTS (see supplementary information). When the central wavelength of the DBR is shifted to lower energies (DBR-520), the dispersion curve is flattened and red shifted while the mode is accessible over a larger in-plane wave vector range (Figure 3.b). In this case it is noticeable that the coupling efficiency is not uniform for all excitation conditions, in fact the mode is weak at normal incidence while the coupling efficiency is stronger for larger

in-plane wave vectors. This effect is due to a fast change of the optical properties of the polymer layer within the wavelength range of the excitonic resonance. Modal excitation at normal incidence (zero-in plane component) is achieved in both multilayer structures (DBR-500, DBR-520). However when the central band of the DBR is at lower energies close to the molecular resonance frequency (as for DBR-585 structure), the modes can only be excited by larger components of the in-plane wavevector.

Optical Tamm States are characterized by a splitting between TE and TM polarized modes that increases quadratically as a function of the in-plane wave-vector[18]. Under illumination at the same incident angle (in-plane wave-vector), the wavelength that matches the mode condition will be larger for the TE mode than for the TM mode. Therefore, in the case of EOTS, for the same photonic structure we should observe different cut-off wavelengths for TE and TM modes. For comparison purposes Figure 4 shows the S-polarized (TE) reflectance maps for the same three EOTS structures. The TM mode of DBR-500 is restricted to a shorter in-plane wavevector range than the TE mode. Interestingly, the designed structures show a clear splitting between TE and TM modes which in some cases might result in a TE or TM only propagation for a particular wavelength. This was seen for the DBR-585 structure where only a TM mode is observed. These results show that it is possible to obtain OTS modes by design with restrictions on polarization and angular directionality by selecting the optical properties of the excitonic materials employed.

In conclusion, we have reported the observation of Excitonic Optical Tamm States using an organic layer as a reflector layer, opening a new route to design tailored photonic modes by harnessing the metal-like properties of heavily dye-doped polymer materials to create all-dielectric nanophotonic structures. EOTS modes with different propagation and polarization conditions were obtained by matching metal-like restricted properties of molecular materials and mode conditions. Such an approach will allow the power of supramolecular chemistry to be harnessed in the design and fabrication of structures to manipulate light in new ways[28], for example using DNA origami [29] The relatively narrow spectral range of

operation might be extended through the use of co-doped thin films containing multiple species [11,30]. Moreover, the use of excitonic materials in nanophotonics leads to a number of intriguing open questions. A potentially attractive benefit over metals is that the detailed properties of these materials may be controlled by optical (and possibly electrical) pumping, perhaps yielding active functionality. Such possibilities also lead us to suggest that these structures might allow other fascinating questions to be addressed, for example what happens to quantum emitters embedded in such materials and whether they might be harnessed for photonic quantum technologies[2].

ASSOCIATED CONTENT

Supporting Information

Reflectance response of thin film molecular reflectors as a function of the reduced oscillator strength. Detailed description of the methods used to obtain the dispersion curves of the Excitonic Optical Tamm States. Analysis of the obtained wavelength cut-off values for both polarized modes (TE, TM).

ACKNOWLEDGMENTS

W.L.B. gratefully acknowledges the support of The Leverhulme Trust and EPSRC (EP/K041150/1).

REFERENCES

(1) Gramotnev, D. K.; Bozhevolnyi, S. I. Plasmonics beyond the Diffraction Limit. *Nat. Photonics* **2010**, *4* (2), 83–91.

(2) Tame, M. S.; McEnery, K. R.; Ozdemir, S. K.; Lee, J.; Maier, S. A.; Kim, M. S. Quantum Plasmonics. *Nat. Phys.* **2013**, *9* (6), 329–340.

(3) Kalusniak, S.; Sadofev, S.; Henneberger, F. ZnO as a Tunable Metal: New Types of Surface Plasmon Polaritons. *Phys. Rev. Lett.* **2014**, *112* (13), 137401.

(4) Naik, G. V; Liu, J.; Kildishev, A. V; Shalaev, V. M.; Boltasseva, A. Demonstration of Al:ZnO as a Plasmonic Component for near-Infrared Metamaterials. *Proc. Natl. Acad. Sci.* **2012**, *109* (23), 8834–8838.

(5) Knight, M. W.; Coenen, T.; Yang, Y.; Brenny, B. J. M.; Losurdo, M.; Brown, A. S.; Everitt, H. O.; Polman, A. Gallium Plasmonics : Deep Subwavelength Spectroscopic Imaging of Single and Interacting Gallium Nanoparticles. *ACS Nano* **2015**, *9* (2), 2049–2060.

(6) Koppens, F. H. L.; Chang, D. E.; García de Abajo, F. J. Graphene Plasmonics: A Platform for Strong Light-Matter Interactions. *Nano Lett.* **2011**, *11* (8), 3370–3377.

(7) Manjavacas, A.; de Abajo, F. J. G. Tunable Plasmons in Atomically Thin Gold Nanodisks. *Nat. Commun.* **2014**, *5*, 3548.

(8) Gentile, M. J.; Núñez-Sánchez, S.; Barnes, W. L. Optical Field-Enhancement and Subwavelength Field-Confinement Using Excitonic Nanostructures. *Nano Lett.* **2014**, *14* (5), 2339–2344.

(9) Gu, L.; Livenere, J.; Zhu, G.; Narimanov, E. E.; Noginov, M. a. Quest for Organic Plasmonics. *Appl. Phys. Lett.* **2013**, *103* (2), 021104.

(10) Anex, B. G.; Simpson, W. T. Metallic Reflection from Molecular Crystals. *Rev. Mod. Phys.* **1960**, *32* (2), 466–476.

(11) Puthumpally-Joseph, R.; Sukharev, M.; Atabek, O.; Charron, E. Dipole-Induced Electromagnetic Transparency. *Phys. Rev. Lett.* **2014**, *113* (16), 163603.

(12) Philpott, M. R.; Brillante, A.; Pockrand, I. R.; Swalen, J. D. A New Optical Phenomenon: Exciton Surface Polaritons at Room Temperature. *Mol. Cryst. Liq. Cryst.* **1979**, *50* (1), 139–162.

(13) Pockrand, I.; Brillante, A.; Philpott, M. R.; Swalen, J. D. Observation of Exciton Surface Polaritons at Room Temperature. *Opt. Commun.* **1978**, *27* (1), 91–94.

(14) Zayats, A. V.; Smolyaninov, I. I.; Maradudin, A. a. Nano-Optics of Surface Plasmon Polaritons. *Phys. Rep.* **2005**, *408* (3-4), 131–314.

(15) Gentile, M. J.; Horsley, S. A. R.; Barnes, W. L. Localized Exciton-Polariton Modes in Dye-Doped Nanospheres: A Quantum Approach. *J. Opt.* **2015**, *18* (1), 015001.

(16) Cacciola, A.; Triolo, C.; Di Stefano, O.; Genco, A.; Mazzeo, M.; Saija, R.; Patanè, S.; Savasta, S. Subdiffraction Light Concentration by J-Aggregate Nanostructures. *ACS Photonics* **2015**, *2* (7), 971–979.

(17) Saikin, S. K.; Eisfeld, A.; Valleau, S.; Aspuru-Guzik, A. Photonics Meets Excitonics: Natural and Artificial Molecular Aggregates. *Nanophotonics* **2013**, *2* (1), 21–38.

(18) Kavokin, A.; Shelykh, I.; Malpuech, G. Lossless Interface Modes at the Boundary between Two Periodic Dielectric Structures. *Phys. Rev. B* **2005**, *72* (23), 233102.

(19) Kaliteevski, M.; Iorsh, I.; Brand, S.; Abram, R.; Chamberlain, J.; Kavokin, a.; Shelykh, I. Tamm Plasmon-Polaritons: Possible Electromagnetic States at the Interface of a Metal and a Dielectric Bragg Mirror. *Phys. Rev. B* **2007**, *76* (16), 165415.

(20) Auguié, B.; Fuertes, M. C.; Angelomé, P. C.; Abdala, N. L.; Soler Illia, G. J. A. A.; Fainstein, A. Tamm Plasmon Resonance in Mesoporous Multilayers: Toward a Sensing Application. *ACS Photonics* **2014**, *1* (9), 775–780.

(21) Badugu, R.; Lakowicz, J. R. Tamm State-Coupled Emission: Effect of Probe Location and Emission Wavelength. *J. Phys. Chem. C* **2014**, *118* (37), 21558–21571.

(22) Symonds, C.; Lheureux, G.; Hugonin, J. P.; Greffet, J. J.; Laverdant, J.; Brucoli, G.; Lemaitre, A.; Senellart, P.; Bellessa, J. Confined Tamm Plasmon Lasers. *Nano Lett.* **2013**, *13* (7), 3179–3184.

(23) Gazzano, O.; de Vasconcellos, S. M.; Gauthron, K.; Symonds, C.; Bloch, J.; Voisin, P.; Bellessa, J.; Lemaître, A.; Senellart, P. Evidence for Confined Tamm Plasmon Modes under Metallic Microdisks and Application to the Control of Spontaneous Optical Emission. *Phys. Rev. Lett.* **2011**, *107* (24), 247402.

(24) Lheureux, G.; Azzini, S.; Symonds, C.; Senellart, P.; Lemaître, A.; Sauvan, C.; Hugonin, J.-P.; Greffet, J.-J.; Bellessa, J. Polarization-Controlled Confined Tamm Plasmon Lasers. *ACS Photonics* **2015**, *2* (7), 842–848.

(25) Yeh, P.; Yariv, A.; Hong, C.-S. Electromagnetic Propagation in Periodic Stratified Media. I. General Theory. *J. Opt. Soc. Am.* **1977**, *67* (4), 438.

(26) Knoester, J. Optical Properties of Molecular Aggregates. In *Proceedings of the International School of Physics "Enrico Fermi". Course CXLIX*; Agranovich, V. M. ;, La Rocca, G. C., Eds.; IOS Press: Amsterdam, 2002; pp 149–186.

(27) López-García, M.; Galisteo-López, J. F.; Blanco, A.; Sánchez-Marcos, J.; López, C.; García-Martín, A. Enhancement and Directionality of Spontaneous Emission in Hybrid Self-Assembled Photonic-Plasmonic Crystals. *Small* **2010**, *6* (16), 1757–1761.

(28) Lehn, J.-M. Toward Complex Matter: Supramolecular Chemistry and Self-Organization. *Proc. Natl. Acad. Sci. U. S. A.* **2002**, *99* (8), 4763–4768.

(29) Wang, M.; Silva, G. L.; Armitage, B. A. DNA-Templated Formation of a Helical Cyanine Dye J-Aggregate. *J. Am. Chem. Soc.* **2000**, *122* (41), 9977–9986.

(30) Würthner, F.; Kaiser, T. E.; Saha-Möller, C. R. J-Aggregates: From Serendipitous Discovery to Supramolecular Engineering of Functional Dye Materials. *Angew. Chemie Int. Ed.* **2011**, *50* (15), 3376–3410.

(31) Johnson, P.; Christy, R. Optical Constants of the Noble Metals. *Phys. Rev. B* **1972**, *6* (12).

Figure 1

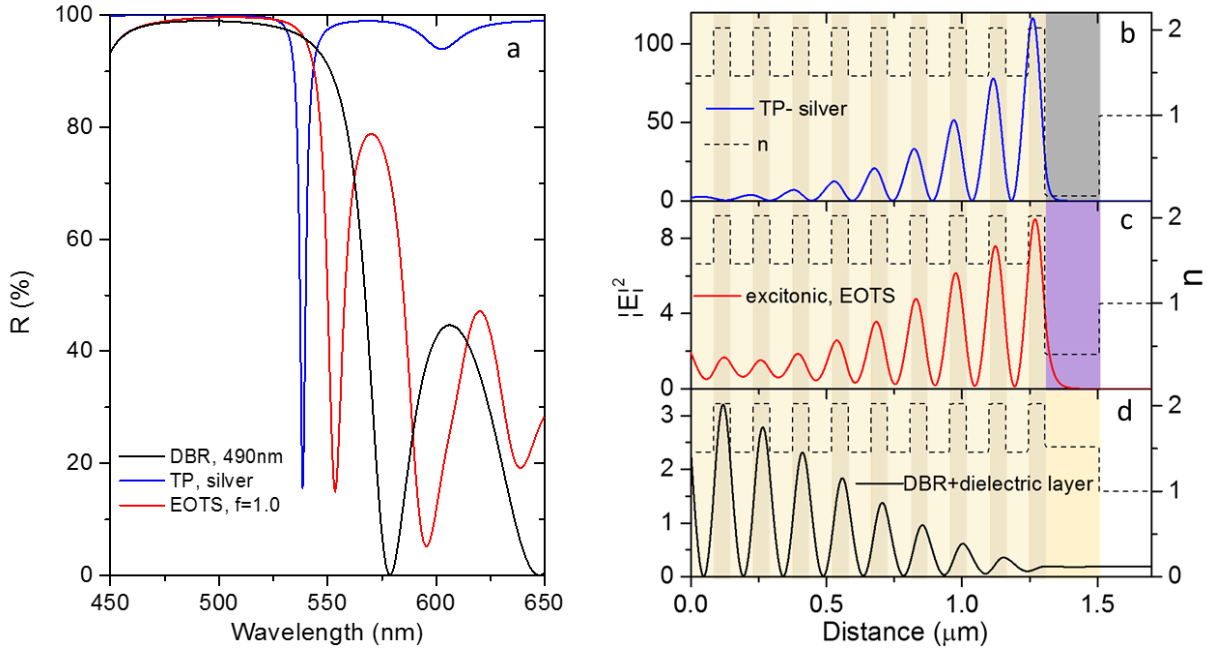

Figure 1. a) Simulated P-polarized (TM) reflection at normal incidence of: a single DBR stack (λ_C=490 nm, black line), an EOTS structure (red line) with an excitonic thin film with an oscillator strength value of 1 and a TP structure (blue line) with silver as metal top layer. Electric field intensity profile in the three structures at normal incidence for: b) TP mode (λ=538 nm, blue line), c) EOTS mode (λ=553 nm, red line), d) stopband region (λ=553 nm, black line). Black dotted lines represent the real part of the refractive index profile. Different colour regions represent the layers with different optical properties. DBR is represented by cream (SiO_2,n=1.46) and light brown (SiN_3, n=2.02). Top layer is shown as grey for silver (n=0.06), lilac for excitonic material (n=0.40) and light yellow as no doped PVA (n=1.52). White colour represents air (n=1).

Figure 2

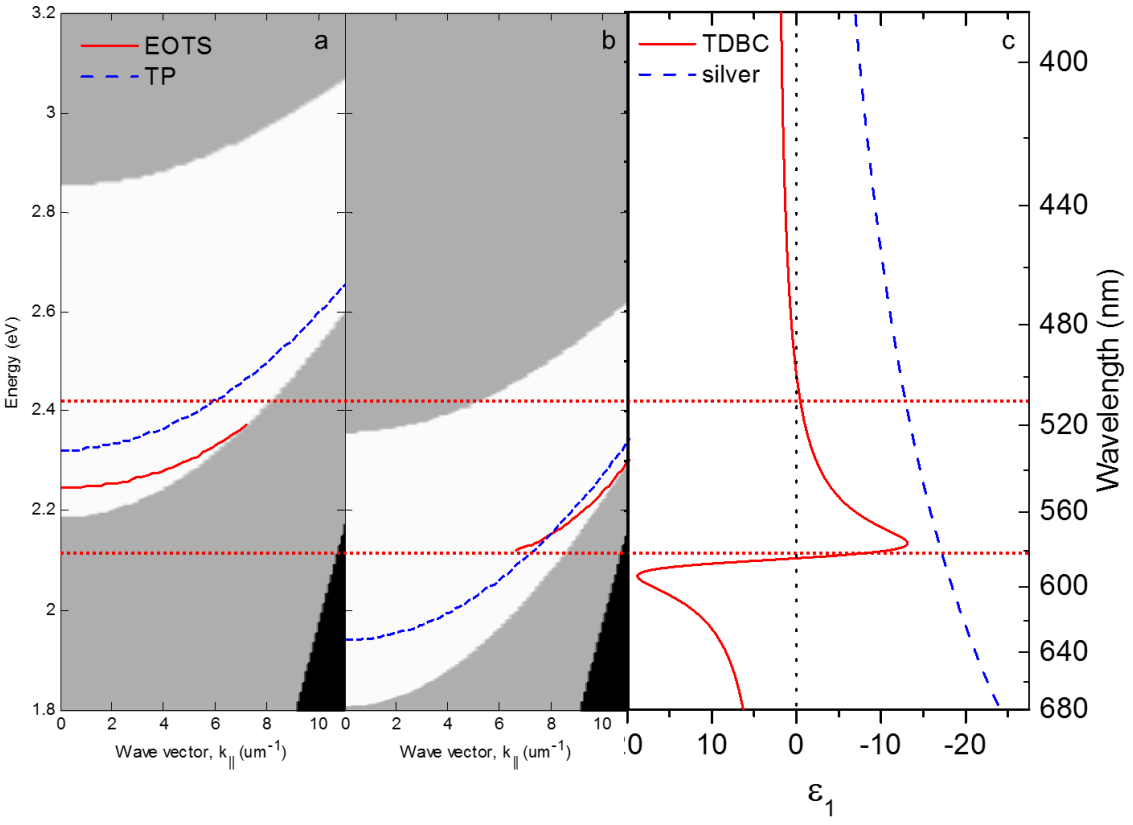

Figure 2. a-b) DBR stop band representation for P-polarized light (TM) for two different DBR's with central wavelengths of 490 nm in 2.a and 590 nm in 2.b. White areas represent the stopband region where the reflectance is higher than 70%. The black regions correspond to areas below the light-line which are not directly accessible by incident light. The grey areas represent all the regions outside the stopband where the reflectance is lower than 70%. Continuous red lines represent the dispersion curves for the EOTS modes supported by the DBR topped with a layer of 200 nm of excitonic material (f_0=1). Blue dashed lines represent the TP dispersion for the same DBR topped by 200 nm of silver. c) Values of the real part of the permittivity for a dielectric medium with an strong resonance at 590 nm and an oscillator strength of 1, and for silver from reference [31]. Red dotted lines mark the spectral region where the real part of the permittivity of the excitonic layer reach negative values of the permittivity.

Figure 3

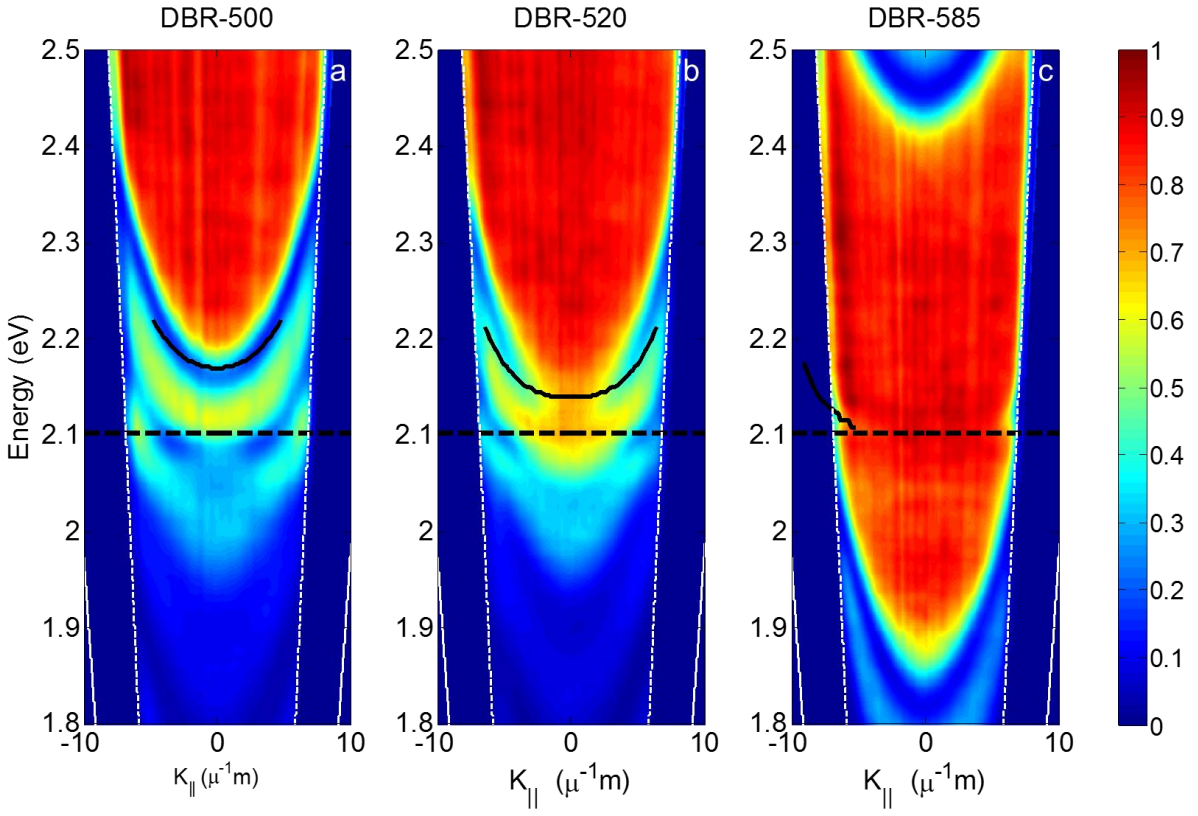

Figure 3. Experimental P-polarized (TM) reflectance maps for: a) EOTS structure composed of a DBR with a central wavelength of 500 nm, b) EOTS structure composed of a DBR with a central wavelength of 520 nm, c) EOTS structure composed of a DBR with a central wavelength of 585 nm. Black line curves corresponds to the calculated dispersion curves for the EOTS TM modes. Black dashed lines indicate the exciton absorption resonance of the J-aggregate molecules at 2.1eV. White dashed lines represent the numerical aperture of the objective used in the reflectance collection and illumination. The continuous white lines correspond to the light cone. In 3.c only the dispersion curve in the negative quadrant is displayed so as to make visualization of the measured features in the positive quadrant of the figure clearer.

Figure 4

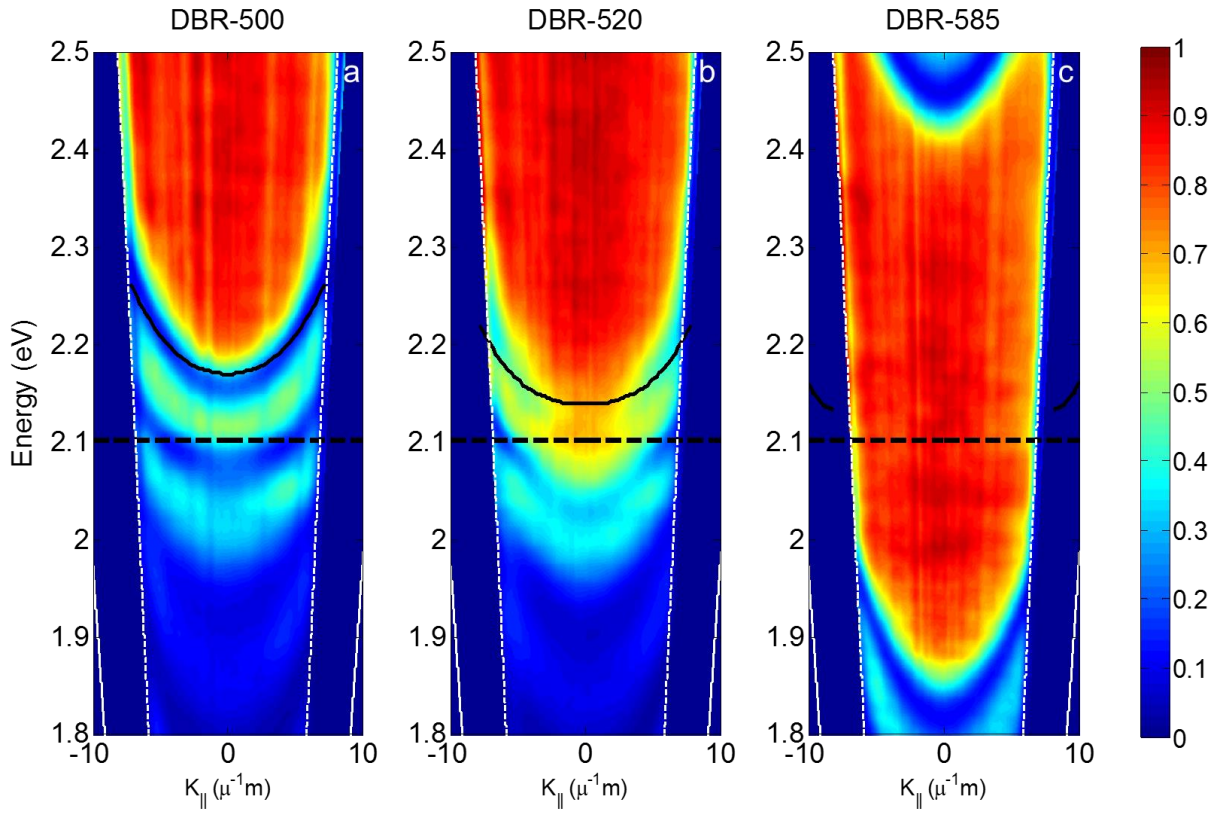

Figure 4. Experimental S-polarized (TE) reflectance maps for: a) EOTS structure composed of a DBR with a central wavelength of 500 nm, b) EOTS structure composed of a DBR with a central wavelength of 520 nm, c) EOTS structure composed of a DBR with a central wavelength of 585 nm. Black line curves corresponds to the calculated dispersion curves for the EOTS TE modes. Black dashed lines indicates the exciton absorption resonance of the J-aggregate molecules at 2.1eV. White dashed lines represent the numerical aperture of the objective use in the reflectance collection and illumination. The continuous white lines correspond to the light cone.